Functional Relevance of Hyper-Reflectivity in Macular Telangiectasia Type 2

Simone Tzaridis[1,2] and Martin Friedlander[1,2]; for the Macular Telangiectasia Type 2-Phase 2 CNTF Research Group

[1]The Lowy Medical Research Institute, La Jolla, California, United States
[2]The Scripps Research Institute, Department of Molecular Medicine, La Jolla, California, United States

Correspondence: Martin Friedlander, The Lowy Medical Research Institute, 3366 N. Torrey Pines Court, La Jolla, CA 92037, USA; friedlan@scripps.edu.

A complete listing of the members of the Macular Telangiectasia Type 2-Phase 2 CNTF Research Group is available in the Appendix.

Received: December 21, 2020
Accepted: February 10, 2021
Published: March 4, 2021

Citation: Tzaridis S, Friedlander M, for the Macular Telangiectasia Type 2-Phase 2 CNTF Research Group. Functional relevance of hyper-reflectivity in macular telangiectasia type 2. *Invest Ophthalmol Vis Sci.* 2021;62(3):6. https://doi.org/10.1167/iovs.62.3.6

Purpose. The purpose of this study was to quantify hyper-reflective lesions on en face optical coherence tomography (OCT) and study its functional relevance in macular telangiectasia type 2 (MacTel).

Design. This was a retrospective, cross-sectional cohort study.

Methods. Baseline image and functional data from participants of a phase II clinical trial (NCT01949324) that studied the effect of Ciliary Neurotrophic Factor in patients with MacTel were analyzed. The projection of hyper-reflectivity within different layers on OCT was used to generate an en face view and measure the en face size of hyper-reflectivity. Ellipsoid zone (EZ)-loss was additionally evaluated, and en face images were superimposed onto microperimetry sensitivity maps, allowing to estimate mean retinal sensitivity within areas displaying hyper-reflectivity and EZ-loss, respectively. Best-corrected visual acuity (BCVA) and reading speed were also analyzed.

Results. Fifty-two eyes from 52 patients were analyzed. Hyper-reflectivity was present in 32 eyes (62%), and EZ-loss in 50 (96%) eyes. Mean lesion size was 0.11 mm^2 (range = 0.01–0.26) for hyper-reflectivity and 0.51 mm^2 (range = 0.02–1.34) for EZ-loss, and lesion sizes correlated strongly (Spearman $r = 0.79$, $P < 0.001$). Although both hyper-reflectivity and EZ-loss were associated with a significant decrease in retinal sensitivity, mean sensitivity thresholds differed significantly between lesions (0.9 dB vs. 16.3 dB; $P < 0.001$), indicating an almost complete loss of sensitivity in hyper-reflective areas. No correlations were found between the size of hyper-reflectivity and BCVA ($r = 0.09$) or reading speed ($r = -0.17$).

Conclusions. En face OCT can be used to quantify the area of hyper-reflective lesions in MacTel. Hyper-reflectivity in MacTel is associated with severe functional impairment, leading to an almost complete loss of retinal sensitivity as observed on microperimetry.

Keywords: macular telangiectasia type 2, hyper-reflectivity, microperimetry, scotomas, optical coherence tomography (OCT)

Macular telangiectasia type 2 (MacTel) is a bilateral, neurodegenerative disease of the central retina with vascular abnormalities and a slowly progressive disease course.[1] Characteristic findings on fundoscopy and multimodal imaging have previously been reported.[1–3] These include decreased retinal transparency, crystalline deposits, and pigment plaques on fundoscopy, and telangiectatic and leaky vessels on fluorescein angiography. On optical coherence tomography (OCT), a disruption of the photoreceptor inner segment-outer segment layer ("ellipsoid zone" [EZ]), hypo-reflective cavities, as well as hyper-reflective lesions and atrophic changes can be observed.[1–3] Typical symptoms include metamorphopsia and reading difficulties,[4–6] whereas distance visual acuity may be relatively preserved.[2,4,7] Reading difficulties have been shown to be associated with paracentral scotomas,[4,8] that may be detected using fundus-controlled perimetry ("microperimetry").[2,4,9] Microperimetry allows the measurement of sensitivity thresholds at specific retinal locations, and the detection and quantification of central and paracentral scotomas. Previous studies demonstrated a correlation between the size of scotomas and the disruption of the EZ on OCT.[10,11] Although the loss of the EZ, its functional correlates, and its role as marker for disease progression have been well studied in MacTel,[4,5,7,10,12,13] little is known about other morphological changes and their functional relevance. Recently, we have described different forms of hyper-reflectivity that represent a common finding on OCT and are associated with disease progression in MacTel.[14] In this study, we quantify hyper-reflective lesions on OCT and study their functional relevance in MacTel.

Methods

Participants

For this retrospective cross-sectional analysis, baseline image and demographic data from participants in a

Investigative Ophthalmology & Visual Science

multicenter clinical trial that studied the effect of ciliary neurotrophic factor (CNTF) on retinal neurodegeneration in patients with MacTel ("A Phase 2 Multicenter Randomized Clinical Trial of CNTF for MacTel"; ClinicalTrials.gov Identifier: NCT01949324) were analyzed. Protocol details of this study have been published previously.[15] The study was conducted according to the tenets of the Declaration of Helsinki, and all participants provided informed consent. In short, the diagnosis of MacTel type 2 was based on characteristic morphologic findings,[1] and confirmed by the central MacTel reading center. Patients underwent a baseline visit including best-corrected visual acuity (BCVA; using Early Treatment Diabetic Retinopathy Study [ETDRS] charts) testing, monocular reading speed testing (using International Reading Speed Texts [IReST]), dilated fundoscopy, color fundus photography (CFP; central 30 degrees), spectral domain-optical coherence tomography (SD-OCT; volume scans of 15 degrees × 10 degrees [high resolution mode, 97 scans, centered on the fovea], Spectralis; Heidelberg Engineering, Heidelberg, Germany), and fundus fluorescein angiography (FFA; 30 degrees, centered on the fovea). Retinal sensitivity was assessed using the Macular Integrity Assessment (MAIA, CenterVue, San Jose, CA, USA) microperimeter. A central test grid with 85 test stimuli (Goldmann size III, with an interstimulus separation ranging between 1 degree for central stimuli and 2 degrees for more eccentric stimuli, 4-2 strategy, 1.27 cd/m^2 background illumination, stimulation time 200 ms, stimulus intensity ranging from 0 to 36 dB) was applied.

For this analysis, only one study visit at baseline and only one eye (either the study eye or fellow eye) per participant was considered. If both eyes of one participant met the inclusion criteria, one eye was randomly selected for analysis. Inclusion criteria were a complete baseline image data set, and sufficient image quality. Exclusion criteria were the presence of neovascular membranes, other retinal diseases, including central serous chorioretinopathy, age-related macular degeneration, or diabetic retinopathy, and previous therapies, including vitreo-retinal surgery, photodynamic therapy, or central laser treatment.

Previously described criteria were applied to identify neovascular membranes on OCT, FFA, and CFP.[14,16]

Hyper-Reflectivity

Hyper-reflectivity on SD-OCT was defined as any hyper-reflective changes located within the inner or outer retinal layers, and exceeding the size of small individual capillaries. Hyper-reflective lesions were further classified into intraretinal and outer retinal hyper-reflectivity. Intraretinal hyper-reflectivity was defined as lesions limited to retinal layers without showing visible connections to the retinal pigment epithelium (RPE) / Bruch's membrane (BM). Outer retinal hyper-reflectivity was defined as lesions extending between retinal layers and the RPE / BM. Crystalline deposits that appear on OCT as small highly reflective spots and are located at the inner surface of the nerve fiber layer[17] were excluded from this definition of hyper-reflectivity.

OCT Analysis

SD-OCT volume scans were used to generate en face images, allowing the measurement of both the size of EZ-loss and the total lesion size of hyper-reflective changes (see Fig. 1). For this purpose, OCT scans were automatically segmented into "all layers" using the manufacturer's software (Heidelberg Eye Explorer, version 1.10.3.0; Heidelberg Engineering), and a manual correction of segmentation lines was applied as needed (minor corrections of segmentation lines were conducted in about 60% of cases). The size of EZ-break was measured as previously described.[18]

The following segmentation lines were used to generate a total of five en face images from five retinal segments using the transverse display within the 3D view panel of the Heidelberg viewer: inner limiting membrane (ILM) to inner plexiform layer (IPL); inner nuclear layer (INL) to outer plexiform layer (OPL); outer nuclear layer (ONL) to photoreceptor inner segments (IS / P1), and photoreceptor outer segments (OS / P2) to BM. Hyper-reflective lesions within each retinal segment were then identified and highlighted using the "draw region" tool on the en face image, and the position of the overlay was checked on corresponding B-scan images.

In a last step, all en face images were superimposed allowing the measurement of the total lesion size of the en face projection of hyper-reflectivity. Additionally, the position and size of EZ-loss was projected and outlined in the same image (see Fig. 1). In the case of multifocal lesions (EZ-breaks and hyper-reflectivity, respectively) the total lesion size was calculated by adding the en face sizes of single lesions.

Color Fundus Photography

CFP images were evaluated for the presence or absence of pigment plaques. CFP images and en face OCT images were superimposed, allowing to compare the position and extent of hyper-reflective and pigmentary changes.

Definition of Functional Impairment and Absolute Scotomas on Microperimetry

On microperimetry, functional impairment ("scotoma") was defined as a decrease of retinal sensitivity of $\geq$ 2 standard deviations (SDs) from an average sensitivity in healthy observers.[19] "Absolute scotomas" were defined as retinal locations at which the highest stimulus intensity could not be seen, resulting in sensitivity thresholds $<$ 0 dB. The size of scotomas was calculated as number of test points within the test field, and was evaluated separately for "absolute scotomas" (number of test points $<$0 dB) and "total scotomas" (number of test points with a decrease in sensitivity of $\geq$2 SDs).

Calculation of Mean Sensitivity Thresholds at Different Retinal Locations

Microperimetry images and OCT en face images were superimposed (see Fig. 2), allowing a direct measurement and comparison of retinal sensitivity thresholds at different retinal locations. Registration of images was performed automatically, as previously described,[20] and the correct alignment and one to one correspondence of images was subsequently verified by an experienced reader. In each eye, mean sensitivity thresholds were calculated within three retinal areas defined as follows: (1) areas showing hyper-reflectivity, (2) areas showing breaks of the EZ, but no hyper-reflectivity, and (3) all test points within the total test field showing neither hyper-reflectivity nor a loss of the EZ (see Fig. 2).

Investigative Ophthalmology & Visual Science

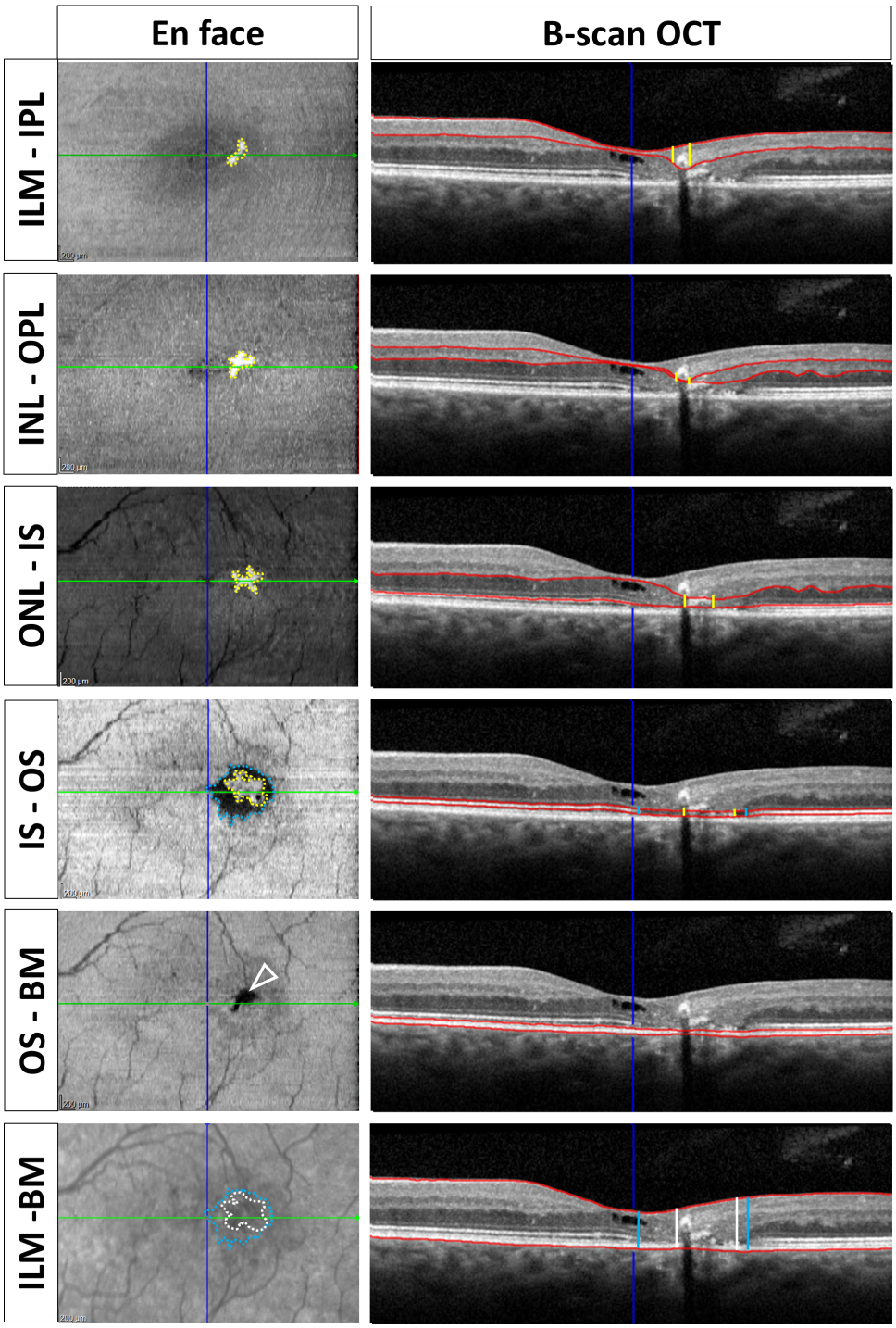

Figure 1. En face projection of hyper-reflectivity and ellipsoid zone (EZ)-loss on optical coherence tomography (OCT). The en face projection of hyper-reflectivity is shown for different retinal layers. *Red lines* indicate the positions of segmentation lines for each layer on B-scan OCT. The *bottom row* shows an overlay of lesions from ILM to BM (*white borderline*) on an infrared image and the corresponding B-scan OCT. Borders of hyper-reflective lesions are indicated by *yellow lines*, areas showing a disruption of the EZ are marked with a *blue borderline*. *Green and dark blue lines* indicate the position of corresponding B-scans on en face images. In the en face illustration of the OS-BM layer shadowing effects from overlying hyper-reflective lesions (*white arrowhead*) are visible. ILM, inner limiting membrane; INL, inner nuclear layer; IPL, inner plexiform layer; ONL,– outer nuclear layer; IS, photoreceptor inner segments; OS, photoreceptor outer segments; BM, Bruch's membrane.

Statistical Analysis

Statistical analysis was performed using R statistical software version 4.0.2. (R Foundation for Statistical Computing, Vienna, Austria). Continuous variables were described by using the mean ± SD and / or median and ranges and categorical variables were analyzed using frequency tables. For intergroup comparisons 1-way ANOVA with

Investigative Ophthalmology & Visual Science

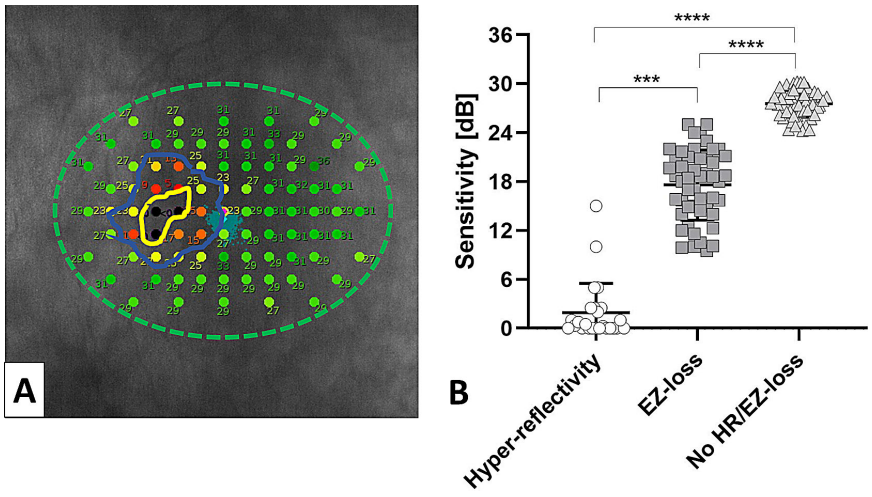

Figure 2. Sensitivity thresholds of the central retina differ significantly between areas with hyper-reflectivity and areas with ellipsoid zone (EZ)-loss. (**A**) Color-coded sensitivity thresholds on microperimetry (in dB) are shown for an exemplary eye. *Black test points* indicate a complete loss (≤0 dB, "absolute scotoma"), and *red, orange, and yellow test points* a relative decrease in sensitivity. *Green test points* represent sensitivity thresholds within normal limits. The en face projections of hyper-reflectivity and EZ-loss are indicated with a *yellow and blue borderline*, respectively. The total test area is marked with a *green-dotted ring*. (**B**) Sensitivity thresholds (mean, single values, and standard deviations [SDs]) at different locations of the central retina (as shown in **A**, and detailed in the main text). ****$P < 0.0001$; ***$P < 0.001$. HR, area displaying hyper-reflectivity; EZ-loss, area displaying EZ-loss, but not hyper-reflectivity; No HR/EZ-loss, area showing neither hyper-reflectivity nor EZ-loss.

Bonferroni correction for multiple testing was computed, unless otherwise indicated. BCVA and reading speed were compared between eyes with and without hyper-reflective changes using the Mann-Whitney test. To test for associations between the en face projection size of hyper-reflectivity and other factors of interest, we used linear multivariate regression. Symmetry on the distribution of hyper-reflectivity projection measures and EZ loss measures was obtained by applying a square root transformation on the data. Significance of each term was assessed using the Wald test. Additionally, Spearman correlation coefficients were used to describe associations between hyper-reflectivity and other parameters of interest, unless otherwise indicated.

A P value < 0.05 was accepted as statistically significant.

Results

Fifty-two eyes from 52 patients (mean age = 59.1 years, range = 47–75; 32 women) were analyzed. Thirty-two eyes (62%) showed hyper-reflectivity with a mean lesion size of 0.11 mm^2 (range = 0.01–0.26). A loss of the ellipsoid zone was present in 50 (96%) eyes, with a mean size of 0.51 mm^2 (range = 0.02–1.34).

Hyper-reflective changes were only observed in eyes showing a break of the EZ, and hyper-reflectivity was limited to areas with EZ-loss. The en face lesion size of hyper-reflectivity and EZ-loss were strongly correlated ($r = 0.79$, $P < 0.001$). Only 4 eyes showed intraretinal hyper-reflectivity, and 28 of 32 eyes showed outer retinal hyper-reflective lesions extending between retinal layers and the RPE / BM. Pigment plaques were observed in 20 of 52 eyes (38%), and coincided in all cases with outer retinal hyper-reflective lesions on OCT. Further characteristics of patients' eyes are detailed in the Table.

Table. Morphological and Functional Measures

Structural Alterations	Mean Values (±SD)*
Size of hyper-reflectivity, mm^2	0.11 (0.11)
EZ-loss area, mm^2	0.51 (0.37)
Size of total scotoma, tp	7.0 (4.7)
Size of absolute scotoma, tp	2.3 (1.4)
Functional measures	
BCVA, total letter score	77.7 (6.0)
Reading speed, wpm	111.0 (50.6)

* Mean values and standard deviations (SDs).

EZ, ellipsoid zone; tp, test point; BCVA, best-corrected visual acuity; wpm, words per minute.

Hyper-Reflectivity and Visual Function

A relative reduction of sensitivity ("total scotomas") was detected in 49 of 52 eyes, and absolute scotomas were found in 21 of 52 eyes. The mean scotoma size was 6.6 test points (range = 1–20 points) for total scotomas, and 2.3 test points (range = 1–7 points) for absolute scotomas.

Absolute scotomas were highly associated with the presence of hyper-reflectivity (in 21/32 eyes with hyper-reflectivity vs. 0/20 eyes without hyper-reflectivity), and the size of hyper-reflectivity correlated strongly with the size of both total scotomas ($r = 0.79$, $P < 0.001$), and absolute scotomas ($r = 0.86$, $P < 0.001$). Notably, this correlation between hyper-reflectivity and absolute scotomas was independent from EZ-loss. The size of EZ-loss correlated best with the size of total scotomas ($r = 0.94$ [vs. correlation with the size of absolute scotomas: $r = 0.79$]). Very small hyper-reflective lesions or EZ-breaks (smaller than a Goldmann size 3 stimulus [0.025 mm]), however, did not necessarily result into a detectable loss of retinal sensitivity. Absolute scotomas were not observed in eyes with hyper-reflective lesions limited to inner retinal layers ($n = 4$). In

Investigative Ophthalmology & Visual Science

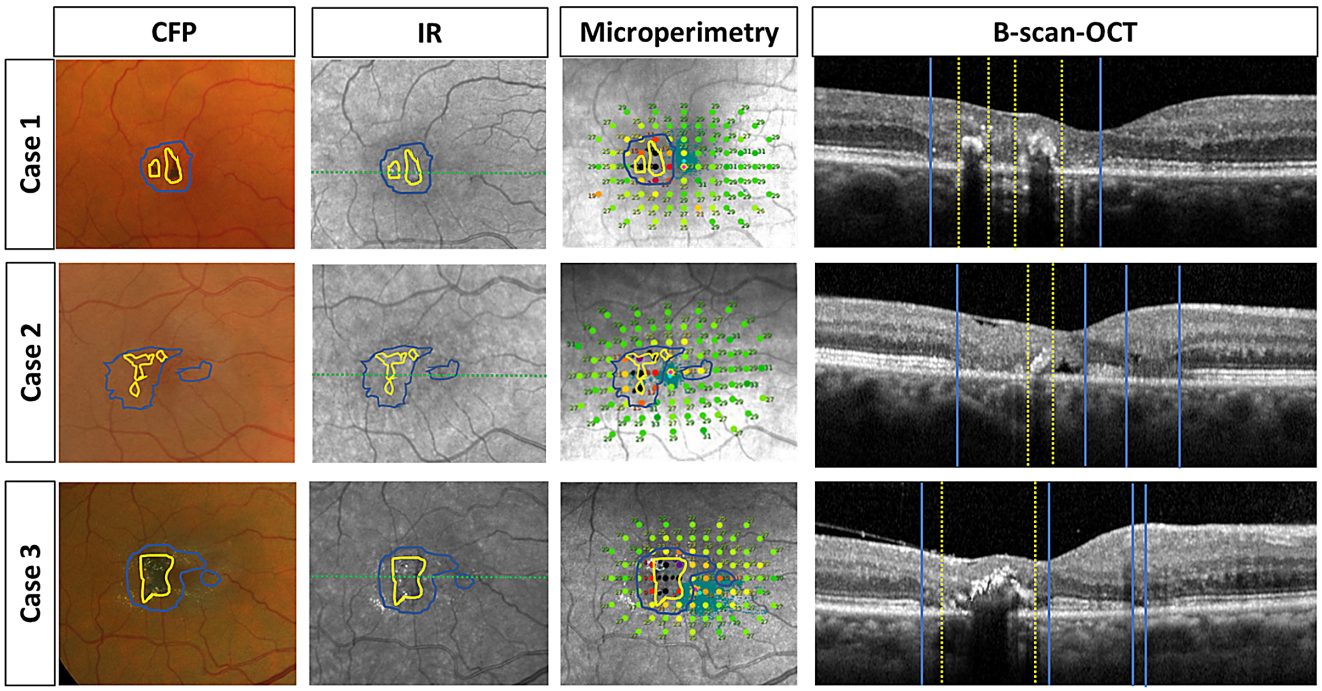

Figure 3. Correlation of scotomas with en face projections of hyper-reflectivity and ellipsoid zone (EZ) loss. Color fundus photography (CFP), infrared (IR) images, microperimetry, and optical coherence tomography (OCT) are shown for three exemplary eyes. Whereas the total scotoma size (summation of *orange, red, and black dots* on microperimetry images) correlates best to areas showing a disruption of the EZ (*blue borders*), absolute scotomas (indicated with *black dots*) seem to correlate to hyper-reflective lesions (*yellow borders*). Hyper-reflective lesions are predominantly observed within areas showing a disruption of the EZ. Pigment plaques as observed on CFP may be associated with hyper-reflective lesions (see cases 1 and 3). The en face projections of hyper-reflectivity and EZ-loss are indicated by a *yellow* and a *blue border* on CFP, IR, and microperimetry, and *yellow and blue lines* indicate the borders of hyper-reflectivity and EZ-loss on B-scan OCTs, respectively. *Green-dotted lines* show the position of OCT-B-scans on IR images.

these eyes, however, hyper-reflective lesions were very small (≤0.01 mm).

Both hyper-reflectivity and EZ-loss were directly associated with a significant decrease in retinal sensitivity. However, sensitivity thresholds differed between lesions. Whereas areas exhibiting a loss of the EZ showed a relative reduction of sensitivity, hyper-reflectivity was associated with an almost complete loss of sensitivity (mean sensitivity thresholds of 16.3 dB vs. 0.9 dB, $P < 0.001$; see Figs. 2, 3). Sensitivity thresholds did not differ between hyper-reflective lesions with and without corresponding pigmentations on CFP. Figure 2 details retinal sensitivity thresholds for different morphological changes. Figure 3 shows overlays of OCT en face images and sensitivity maps, indicating a direct correlation of hyper-reflectivity and EZ-loss with functional impairment on microperimetry.

No correlations were found between the size of hyper-reflectivity and BCVA ($r = 0.09$) or reading speed ($r = -0.17$). BCVA and reading speed did not differ significantly between eyes with and eyes without hyper-reflectivity (BCVA = 79 letters [median; range = 71–92] vs. 76 letters [median, range = 60–91], $P = 0.28$; and reading speed: 96 words per minute [wpm; median, range = 27–186 wpm] vs. 117 wpm [median, range = 8–214 wpm], $P = 0.18$), and no significant differences were found between the right eyes and left eyes. Results from the multivariate regression analysis are detailed in Supplementary Table S1. Supplementary Figure S1 illustrates correlations between the size of hyper-reflectivity and different morphological and functional measures.

Discussion

Hyper-reflectivity refers to an abnormal, disease-associated focal increase in reflectivity signaling on OCT. Previous studies have described hyper-reflective changes and discussed their anatomic correlates in MacTel. The latter include pigmentary changes, possibly deriving from migrating RPE-cells, neurodegenerative processes, cellular debris, and vascular alterations.[21–23] Although a correlation of hyper-reflectivity with disease progression has been proposed, its functional relevance has yet not been evaluated. In this study, we used an approach that quantified hyper-reflective changes in MacTel. The projection of hyper-reflective lesions in an en face view of the retina on OCT allowed an exact point-wise correlation with microperimetry data, and a quantification of the en face projection size of hyper-reflective lesions. A limitation of this approach is that it does not consider the in-depth extension of hyper-reflectivity within different retinal layers. We hypothesized, however, that hyper-reflectivity might interfere with incoming light and impede vertical signal transmission within the retina. Thus, the projection of hyper-reflectivity in an en face view would also allow the visualization of functional impairment in one plane. Similar observations have been previously reported in eyes with hyper-reflective lesions associated with retinal angiomatous proliferation (RAP). In these eyes, the development of a vascular net in the inner layers of the retina has been proposed to cause early functional impairment and dense scotomas.[24]

In this study, we found a direct correlation between hyper-reflectivity and a severe, almost complete loss of retinal sensitivity ("absolute scotomas"). Areas displaying a loss of the EZ, on the other hand, correlated with a relative reduction of retinal sensitivity. Our observations are consistent with recent findings showing that a loss of the EZ is better correlated with the total than with the absolute scotoma size alone.[18]

Typical symptoms that have been shown to be associated with paracentral scotomas in MacTel are reading difficulties[4] and an impairment of stereoscopic function.[25] Central visual acuity, however, may be relatively preserved due to the paracentral nature of structural changes.[4,6] In line with these findings, we observed no correlation between hyper-reflective changes and BCVA. The majority of hyper-reflective lesions were limited to the temporal parafovea. We observed broad lesions, extending to the fovea and nasal parafovea only in eyes with advanced disease stages. In these cases, a drop in central visual acuity was noted. Although reading performance was overall impaired in our patients, a direct correlation between reading speed and the en face size of hyper-reflective lesions and associated absolute scotomas was not observed. Results from a previous study evaluating binocular reading and its correlation with scotoma characteristics suggested an association of absolute scotomas with a drop in reading acuity in MacTel.[8] Although our current analysis did not reveal significant differences in reading performance between eyes with and without hyper-reflective lesions, a slight drop in reading speed could be observed with the occurrence of hyper-reflective changes and associated absolute scotomas. Based on our findings from this and previous studies,[8] we concluded that additional parameters and scotoma characteristics that have not been considered in this analysis, might have impacted patients' reading performance more severely. These factors may include eye laterality (right eyes versus left eyes, and projection of scotomas in reading direction) and the size and position of total scotomas in relation to the fovea.[4,8]

Previously, different structural changes have been observed to correlate with absolute scotomas on microperimetry in diseases affecting the central retina. These included retinal pigment epithelium atrophy, photoreceptor degeneration, chorioretinal scars, subretinal hemorrhages, and choroidal neovascularization.[26] Our analysis mainly focused on inner and outer retinal hyper-reflective lesions as typical morphological alteration in MacTel. Neovascular membranes, fibrosis, and hemorrhages were excluded. An association of outer retinal hyper-reflective lesions with a degeneration of photoreceptors and/ or RPE is conceivable, given that these lesions were in all cases associated with a disruption of the EZ / photoreceptor layer, and, in some cases, with additional structural changes of the RPE (e.g. focal detachments). A loss of the EZ alone, however, was associated with less severe functional impairment, indicating an additional disruptive impact of hyper-reflectivity on retinal function. Based on recent OCT-angiography (OCT-A) studies, associations of hyper-reflective lesions with changes in blood flow have been proposed in MacTel.[14,27] In this context, different vascular abnormalities have been described, including the formation of retinal-retinal and retinal-choroidal anastomoses. Although the lack of OCT-A data in this study does not allow for a direct correlation among vascular changes, hyper-reflective lesions, and retinal function, a vascular component may have contributed to the observed functional impairment. As stated above, similar findings have been described in eyes with RAP lesions, where intraretinal vascular complexes were proposed to block incoming light and interfere with intraretinal signal transmission.[24]

Interestingly, no differences in sensitivity thresholds were observed between hyper-reflective lesions with and without accumulations of pigment plaques on CFP, indicating that pigmentary changes did not additionally impede retinal function.

Notably, hyper-reflective lesions limited to inner retinal layers were overall rare, and, when observed, did not show functional correlates on microperimetry. Different explanations for this observation are conceivable. Either lesion sizes were too small to result in a detectable functional loss on microperimetry, or anatomic correlates associated with this type of lesion are different, and thus not necessarily associated with functional loss. Histological studies might help to identify the anatomic and pathophysiological basis for hyper-reflectivity in MacTel, and thus explain the associated functional impairment we observed in this study.

This study has several limitations, including its retrospective approach, cross-sectional character, and limited numbers. The study population was preselected according to the inclusion and exclusion criteria of the CNTF trial that only considered eyes with moderate disease stages. Thus, early and late stages were under-represented, and the observed distributions and prevalence rates of hyper-reflectivity and disease stages were not representative for the broader MacTel population.

Conclusions

We present a methodological approach that allows the quantification of the area of hyper-reflective lesions on en face OCT in MacTel. The en face projection of hyper-reflectivity enables a direct correlation with retinal function as evaluated by microperimetry. We demonstrate that hyper-reflectivity in MacTel is associated with severe functional impairment, resulting in an almost complete (para)central loss of retinal sensitivity.

Acknowledgments

The authors thank Roberto Bonelli for his statistical advice.

Supported by the Lowy Medical Research Institute, La Jolla, CA, USA; The funding organizations had no role in the design or conduct of the experiments.

Disclosure: **S. Tzaridis**, None; **M. Friedlander**, None

References

1. Charbel Issa P, Gillies MC, Chew EY, et al. Macular telangiectasia type 2. *Prog Retin Eye Res*. 2013;34:49–77.
2. Charbel Issa P, Helb HM, Rohrschneider K, Holz FG, Scholl HP. Microperimetric assessment of patients with type 2 idiopathic macular telangiectasia. *Invest Ophthalmol Vis Sci*. 2007;48(8):3788–3795.
3. Barthelmes D, Gillies MC, Sutter FK. Quantitative OCT analysis of idiopathic perifoveal telangiectasia. *Invest Ophthalmol Vis Sci*. 2008;49(5):2156–2162.
4. Finger RP, Charbel Issa P, Fimmers R, Holz FG, Rubin GS, Scholl HP. Reading performance is reduced by parafoveal

scotomas in patients with macular telangiectasia type 2. *Invest Ophthalmol Vis Sci*. 2009;50(3):1366–1370.
5. Charbel Issa P, Holz FG, Scholl HP. Metamorphopsia in patients with macular telangiectasia type 2. *Doc Ophthalmol*. 2009;119(2):133–140.
6. Heeren TF, Holz FG, Charbel Issa P. First symptoms and their age of onset in macular telangiectasia type 2. *Retina*. 2014;34(5):916–919.
7. Heeren TF, Clemons T, Scholl HP, et al. Progression of vision loss in macular telangiectasia type 2. *Invest Ophthalmol Vis Sci*. 2015;56(6):3905–3912.
8. Tzaridis S, Herrmann P, Charbel Issa P, et al. Binocular inhibition of reading in macular telangiectasia type 2. *Invest Ophthalmol Vis Sci*. 2019;60(12):3835–3841.
9. Trauzettel-Klosinski S. Reading disorders due to visual field defects: a neuro-ophthalmological view. *Neuro-Ophthalmology*. 2002;27(1-3):79–90.
10. Heeren TFC, Kitka D, Florea D, et al. Longitudinal correlation of ellipsoid zone loss and functional loss in macular telangiectasia type 2. *Retina*. 2018;38(Suppl 1):S20–S26.
11. Sallo FB, Peto T, Egan C, et al. "En face" OCT imaging of the IS/OS junction line in type 2 idiopathic macular telangiectasia. *Invest Ophthalmol Vis Sci*. 2012;53(10):6145–6152.
12. Sallo FB, Leung I, Mathenge W, et al. The prevalence of type 2 idiopathic macular telangiectasia in two African populations. *Ophthalmic Epidemiol*. 2012;19(4):185–189.
13. Charbel Issa P, Troeger E, Finger R, Holz FG, Wilke R, Scholl HP. Structure-function correlation of the human central retina. *PLoS One*. 2010;5(9):e12864.
14. Tzaridis S, Hess K, Heeren TFC, Bonelli R, Holz FG, Friedlander M. Hyper-reflectivity on optical coherence tomography in macular telangiectasia type 2. [published online ahead of print January 6, 2021]. *Retina*, https://doi.org/10.1097/IAE.0000000000003111.
15. Chew EY, Clemons TE, Jaffe GJ, et al. Effect of ciliary neurotrophic factor on retinal neurodegeneration in patients with macular telangiectasia type 2: a randomized clinical trial. *Ophthalmology*. 2019;126(4):540–549.
16. Heeren TFC, Chew EY, Clemons T, et al. Macular telangiectasia type 2: visual acuity, disease end stage, and the MacTel area: MacTel Project Report Number 8. *Ophthalmology*. 2020;127(11):1539–1548.
17. Sallo FB, Leung I, Chung M, et al. Retinal crystals in type 2 idiopathic macular telangiectasia. *Ophthalmology*. 2011;118(12):2461–2467.
18. Heeren TFC, Kitka D, Florea D, et al. Longitudinal correlation of ellipsoid zone loss and functional loss in macular telangiectasia type 2. *Retina*. 2018;38(Suppl 1):S20–S26.
19. Molina-Martin A, Pinero DP, Perez-Cambrodi RJ. Normal values for microperimetry with the MAIA microperimeter: sensitivity and fixation analysis in healthy adults and children. *Eur J Ophthalmol*. 2017;27(5):607–613.
20. Matsopoulos GK, Asvestas PA, Mouravliansky NA, Delibasis KK. Multimodal registration of retinal images using self organizing maps. *IEEE Trans Med Imaging*. 2004;23(12):1557–1563.
21. Tzaridis S, Heeren TFC, Mai C, et al. Right-angled vessels in macular telangiectasia type 2 [published online ahead of print February 26, 2021]. *Br J Ophthalmol*, https://doi.org/10.1136/bjophthalmol-2018-313364.
22. Leung I, Sallo FB, Bonelli R, et al. Characteristics of pigmented lesions in type 2 idiopathic macular telangiectasia. *Retina*. 2018;38(Suppl 1):S43–S50.
23. Baumuller S, Charbel Issa P, Scholl HP, Schmitz-Valckenberg S, Holz FG. Outer retinal hyperreflective spots on spectral-domain optical coherence tomography in macular telangiectasia type 2. *Ophthalmology*. 2010;117(11):2162–2168.
24. Midena E, Pilotto E. Microperimetry in age: related macular degeneration. *Eye (Lond)*. 2017;31(7):985–994.
25. Muller S, Heeren TFC, Nadal J, et al. Stereoscopic vision in macular telangiectasia type 2. *Ophthalmologica*. 2019;241(3):121–129.
26. Tezel TH, Del Priore LV, Flowers BE, et al. Correlation between scanning laser ophthalmoscope microperimetry and anatomic abnormalities in patients with subfoveal neovascularization. *Ophthalmology*. 1996;103(11):1829–1836.
27. Breazzano MP, Yannuzzi LA, Spaide RF. Characterizing retinal-choroidal anastomosis in macular telangiectasia type 2 with optical coherence tomography angiography. *Retina*. 2020;40(1):92–98.

Appendix: MacTel NTMT-02 Research Group

National Eye Institute (NEI)

Emily Y. Chew, MD, Clinical Project Director

Joint Steering Committee

John Fanning (Chair)
Martin Friedlander, MD, PhD
Emily Chew, MD
Alan Bird, MD
Charles A. Johnson, MB, ChB
Traci Clemons, PhD
Richard Small

Data Safety & Monitoring Committee

David C. Musch, PhD, MPH (Chair), University of Michigan, Kellogg Eye Center
David J. Wilson, MD, Oregon Health and Science University
Harry W. Flynn Jr., MD, Bascom Palmer Eye Institute

Neurotech Pharmaceuticals, Inc.

Charles A. Johnson, MB, ChB, Chief Medical Officer
Jenni Bursell, Clinical Project Manager
John Duggan, Quality Assurance

Lowy Medical Research Institute

Jennifer Trombley, RN, MSN, CCRC, Director, Clinical Operations
Martin Friedlander, MD, PhD, President
Anton Lever, Group Manager, Finance
John Fanning, Finance Director

Duke Reading Center

Glenn Gaffe, MD, Director
Shashi Kini, Project Manager
Justin Myers, IT Technical Analyst
Elenora Lad, MD, Ophthalmologist
Sina Farsiu, PhD, Ophthalmology

Moorfields Reading Center

Tunde Peto, MD, PhD (Former Director)
Ferenc Sallo, MD, PhD (Ophthalmologist)

The Coordinating Center: The Emmes Corporation

Traci Clemons, PhD, Principal Investigator

Investigative Ophthalmology & Visual Science

Sarah Duwel, RN, MA, CCRA Project Director
Sherrie Schenning, CRA
Traci Scheer, Data Manager
Lena Bradley, Protocol Monitor
Radhika Kondapaka, Safety Monitor
Robert Lindblad, MD, Chief Medical Officer
Alexa Irazabal, Administrative Coordinator
George Lindblad, Computer Systems Analyst

Novotech – Australia

Lyn Corrigan, Project Manager
Katrina Norial, Monitor

ERG Grading

Neal Peachey, MD, ERC Grading Consultant

Adaptive Optics Imaging

Arshia Mian – University of California, San Francisco
Jacque L. Duncan, MD – University of California San Francisco
Austin Roorda, PhD – University of California, Berkley
Mina Chung, MD – University of Rochester
Lisa Latchney – University of Rochester
David Williams, PhD – University of Rochester
Joseph Carroll, PhD – The Medical College of Wisconsin

(002) Centre for Eye Research Australia

Robyn Guymer, MB, BS, PhD, FRANZCO (Site PI)
Penny Allen, MD (Ophthalmologist)
Robert Finger, MD (Former Ophthalmologist)
Thanh Nguyen, MD (Ophthalmologist)
Sukhpal Sandhu, MD (Ophthalmologist)
Shilpa Taori, MD (Former Ophthalmologist)
Sanjeewa Wickremasinghe, MD (Ophthalmologist)
Hessom Razavi (Ophthalmologist)
Jonathan, Yeoh, MD (Ophthalmologist)
Tania Cipriani (Former Clinic Coordinator)
Maria Kolic (Photographer)
Melinda Cain (Clinic Coordinator)
Richard Smallwood (Photographer)
Andrew Newton (Photographer)
Chi Luu (ERG Technician)
Fleur O'Hare (Ophthalmic Technician)
Elizabeth Baglin (Ophthalmic Technician)
Pyrawy Sivarajah (Ophthalmic Technician)
Kate Brassington (Ophthalmic Technician)
Khin-Zaw Aung (Ophthalmic Technician)
Emily Caruso (Clinic Coordinator)

(005) Jules Stein Eye Institute

Jean-Pierre Hubschman, MD (Site PI)
Steven Schwartz, MD (Ophthalmologist – Sub-Investigator)
Gad Heilweil, MD (Ophthalmologist – Sub-Investigator)
Hamid Hosseini, MD (Ophthalmologist – Sub-Investigator)
David Cupp, MD (Ophthalmologist – Former Sub-Investigator)
Joshua Udoetuk, MD (Ophthalmologist – Former Sub-Investigator)
Ryan Wong, MD (Ophthalmologist – Former Sub-Investigator)
Sujit Itty, MD (Ophthalmologist – Former Sub-Investigator)
Christian Sanfilippo, MD (Ophthalmologist – Sub-Investigator)
Sanket Shah, MD (Ophthalmologist – Sub-Investigator)
Elizabeth Richter, MD (Ophthalmologist – Former Sub-Investigator)
Robert Lalane, MD (Ophthalmologist – Former Sub-Investigator)
Michael Klufus, MD (Ophthalmologist – Former Sub-Investigator)
Aaron Nagiel, MD, PhD (Ophthalmologist – Former Sub-Investigator)
Nina Zelcer (Study Coordinator)
Rosaleen Ostrick, MPH, MA (Study Coordinator)
Jennie Kageyama, OD (Ophthalmic Technician)
Melissa Chun, OD (Ophthalmic Technician)
Steven Nusinowitz, PhD (ERG Technician)
Logan Hitchcock (Former Study Coordinator Data Entry)
Lauren Eash (Photographer)
Maria Castro, RN (FA Injection)
Nilo Davila (Former Photographer)
Rene Obispo (Photographer)
Orly Catz (Photographer)
Sara Harmon (MAIA Technician)
Paul Paquette (Photographer)
Bita Shuku, OD (Ophthalmic Technician)
Joshua Koo (Photographer)

(006) Lions Eye Institute

Ian Constable, MB, BS, FRANZCO, FRACS (Site PI)
Fred Chen, MB, BS, PhD, FRANZCO (Ophthalmologist)
Susan Irwin, PA
Antonia Busby (Clinic Coordinator)
Diana Bowman (Clinic Coordinator)
Kate Maslin (Former Clinic Coordinator)
Anne McSweeney (Ophthalmic Technician)
Chris Barry (Photographer)
Ivy Tang (Photographer)
Max Cuyers (Ophthalmic Technician)
Frank Shilton (Photographer)
Sharon Radtke (Data Entry)
Mary Cheng (Photographer)
Robert Cowles (Data Entry)
Gareth Lingham (Photographer)
Holly Brown (Photographer)

(009) National Eye Institute

Henry Wiley, MD (Site PI and Ophthalmologist)

Investigative Ophthalmology & Visual Science

Katherine Hall, RN, COT, MSN (AI and Lead Study Coordinator)
Emily Chew, MD (Lead AI and Ophthalmologist)
Catherine Cukras, MD, PhD (AI and Ophthalmologist)
Wai Wong, MD, PhD (AI and Ophthalmologist)
Brett Jeffrey, PhD (AI and Staff Scientist)
Denise Cunningham, MS, Med, FOPS (Lead Photographer)
Michael Bono, CRA, COT (Ophthalmic Photographer)
Mike Arango (Ophthalmic Photographer)
Leanne Reuter, MS, COA (Ophthalmic Technician)
Dessie Koutsandreas, BA, COA (Ophthalmic Technician)
Roula Nashwinter, COT (Ophthalmic Technician)
Darryl Hayes, COT (Ophthalmic Technician)
Enilo Balant, COMT (Ophthalmic Technician)
Patrick Lopez, COT (Ophthalmic Technician)
John Rowan, COMT (Ophthalmic Technician)
Christina Appleman, COMT (Ophthalmic Technician)
Sharon Yin, COMT (Ophthalmic Technician)
Hope DeCederfelt, RPh (Pharmacist)
Penelope Friedman, MD (Internal Medicine)
Stacey Solin, RN, NP (Internal Medicine)

(010) Retina Associates of Cleveland, Inc.

Lawrence J. Singerman, MD (Site PI)
Jerome P. Schartman, MD (Surgeon)
Scott Pendergast, MD (Ophthalmologist)
David Miller, MD (Surgeon)
Hernando Zegarra (Ophthalmologist)
George Michael Carson, PA-C (Surgical Assistant)
Joseph M. Coney, MD (Ophthalmologist)
Michael Novak, MD (Ophthalmologist)
Llewelyn Rao, MD (Ophthalmologist)
Susan Rath, PA-C (Ophthalmic Technician)
Jenny Peck, PA-C (Surgical Assistant)
Michelle James, PA-C (Surgical Assistant)
Gregg Greanoff (CRA) (Photographer)
John Dubois (CRA) (Photographer)
Vivian Tanner (COT) (Photographer)
Dianne Himmelman, RN (Ophthalmic Technician)
Diane Weiss, RN (Clinic Coordinator)
Jannie Arouri (Study Drug Processing)
Tia Drugen (Ophthalmic Technician)
Cecelia Rykena (Ophthalmic Technician)

(011) Save Sight Institute

Mark Gillies (Site PI)
Alex Huynor
Samantha Fraser-Bell
Penny Allen, MD (Ophthalmologist)
Anagha Vaze, MD (Former Ophthalmologist)
Richard Symes, MD (Ophthalmologist)
Luke Seesink (Clinic Coordinator)
Aaron Joe, MD (Ophthalmologist)
Eline Whist, MD (Ophthalmologist)
Maria Williams (Clinic Coordinator)
Susan Chin (Former Clinic Coordinator and Photographer)
Ajaya Jadhav (Former Clinic Coordinator and HVF Technician)
Haipha Ali (Photographer)
Stephanie Goodwin (Former Photographer)
Christine Gaston (Former Ophthalmic Technician)
Amparo Herrera Bond (Photographer)
Nonna Saakova (ERG Technician)
Maria Korakov (ERG Technician)
Sophia Zagora (Former Ophthalmologist)
Annabel Senior (Former Clinic Coordinator)
Hemal Mehta (Former Ophthalmologist)
Kristy Francis (Former Photographer)
Kathryn Llewelyn (Former Photographer)
Shereen Lobb
Aaron Yeung (Former Ophthalmologist)
Trevor Wilson (Physical Examinations)
Priyanka Verma-Sehgal (Former Clinic Coordinator and Photographer)
Sharon McKenzie (Clinic Coordinator)
Roxy Medina (Clinic Coordinator)
Jaclyn Bryant (Photographer)
Bareen Pordilly (Former Photographer)
Amanda Dinh (Photographer)

(019) University of Michigan, Kellogg Eye Center

Grant Comer, MD (Site PI)
Pamela Campbell, COT, CCRP (Clinic Coordinator)
Lindsay Godsey, MS, COA, CCRP (Ophthalmic Technician)
Rob Prusak, CRA (Photographer)
Linda Fournier, COA (Ophthalmic Technician)
Tim Steffens, CRA (Photographer)
Linda Goings, CRA (Photographer)
Moella Hesselgrave, COA Former (Ophthalmic Technician)
Callie Gordon, COT Former (Ophthalmic Technician)
Tiffany Craig-Buers, COT Former (Ophthalmic Technician)
Hillary Bernard, CRA Former (Photographer)
Rebecca Brown, COA Former (Ophthalmic Technician)
Timothy Costello (Photographer)

(020) University of Wisconsin

Barbara Blodi, MD (Site PI)
Michael Ataweel, MD (Ophthalmologist)
Justin Goltlieb (Ophthalmologist)
Kris Dietzman (Clinic Coordinator)
Angie Wealti (Ophthalmic Technician)
John Peterson (Former Photographer)

Investigative Ophthalmology & Visual Science

Denise Krolnik (Photographer)
Sandie Reed (Photographer)
Jennie Perry-Raymond (Former Photographer)
Chris Smith (Photographer / Ophthalmic Technician)

(026) Bascom Palmer Eye Institute

Philip Rosenfeld, MD (Site PI)
Cristina M. Lage-Rodriguez (Clinic Coordinator)
Monica Arango (Clinic Coordinator)
Thomas Albini, MD (Ophthalmologist)
Jamey Hammond (Ophthalmic Technician)
Maria Y. Esquiabro (Clinic Coordinator)
Elizabeth Sferza Camp (Ophthalmic Technician)
Jim Oramas (Photographer)
Giselle DeOliveira (Photographer)
Zohar Yehoshua, MD (Ophthalmologist)
Ninel Gregori, MD (Ophthalmologist)
Brandon Sparling (Photographer)
Janet Davis, MD (Ophthalmologist)
Belen Rodriguez (Clinic Coordinator)
Alexey Gomez Rodriguez (Ophthalmic Technician)
Ivonne Camps (Ophthalmic Technician)
Linda O'Koren (OCT Technician)

(027) Massachusetts Eye and Ear

Dean Eliott, MD (Site PI)
Ivana Kim, MD (Ophthalmologist)
Joan W. Miller, MD (Ophthalmologist)
Hua Lu, MD (Internist)
Patricia Houlihan (Study Coordinator)
Ursula Bator, OD (Optometrist)
Charlene Callahan (Former Photographer)
Matthew DiRocco (Photographer)
Marcia Grillo (Former Photographer)
John Head (Former Photographer)
Meredith Ryan (Clinic Coordinator)
Deeba Hussain, MD (Ophthalmologist)
Norm Simonton (HVF Technician)
Yehbinda Ambrose (HVF Technician)
John Miller, MD (Ophthalmologist)
Christine Finn (IP Handling, Pharmacist)
George Papaliodis, MD (Internist)
Ann Pappadopoulos (IP Handling, Pharmacist)
Judy Yee (IP Handling, Pharmacist)
Shyana Harper (Former Clinic Coordinator, Clinical Research Supervisor)
Kiran Chaudhary (Former Clinical Research Supervisor)
Anneliese Koleber (Ophthalmic Technician)
Sarah Brett (Photographer)

(028) Emory University

Jiong Yan, MD (Site PI)
Timothy Olson, MD (Ophthalmologist)
Donna Leef (Clinic Coordinator)
Jannah Dobbs, CRA (Photographer)
Matthew Raeber, CRA (Photographer)
Deborah Gibbs, COMT (Ophthalmic Technician)
Lindy DuBois (Ophthalmic Technician)
Joel Chasen, MD (Ophthalmologist)
Matthew Debiec, MD (Ophthalmologist)

Investigative Ophthalmology & Visual Science